

DIMMING OF THE MID-20TH CENTURY SUN

PETER FOUKAL

192 Willow Rd., Nahant, MA 01908, USA; pvfoukal@comcast.net
Received 2015 August 13; accepted 2015 October 27; published 2015 December 2

ABSTRACT

Area changes of photospheric faculae associated with magnetic active regions are responsible for the bright contribution to variation in total solar irradiance (TSI). Yet, the 102-year white light (WL) facular record measured by the Royal Greenwich Observatory between 1874 and 1976 has been largely overlooked in past TSI reconstructions. We show that it may offer a better measure of the brightening than presently used chromospheric proxies or the sunspot number. These are, to varying degrees, based on magnetic structures that are dark at the photosphere even near the limb. The increased contribution of the dark component to these proxies at high activity leads to an overestimate of solar brightening around peaks of the large spot cycles 18 and 19. The WL facular areas measure only the bright contribution. Our reconstruction based on these facular areas indicates that TSI decreased by about 0.1% during these two cycles to a 20th century *minimum*, rather than brightening to some of the highest TSI levels in four centuries, as reported in previous reconstructions. This TSI decrease may have contributed more to climate cooling between the 1940s and 1960s than present modeling indicates. Our finding adds to previous evidence that such suppression of solar brightening by an increased area of dark flux tubes might explain why the Sun is anomalously quiet photometrically compared to other late-type stars. Our findings do not change the evidence against solar driving of climate warming since the 1970s.

Key words: solar–terrestrial relations – Sun: activity – Sun: faculae, plages

1. INTRODUCTION

Information on total solar irradiance (TSI) variation prior to the beginning of space-borne measurements in 1978 is based on reconstructions of the dimming by sunspots and brightening by smaller-diameter magnetic flux tubes observed near the photospheric limb as the white light (WL) faculae. Dimming by spots can be reconstructed from their projected areas measured since 1874 and their relatively well known photometric contrast. But it is harder to reconstruct the bright component of TSI variation because the faculae are easily observable only near the solar limb and their small size makes contrast measurements difficult.

A regression technique in which the facular areas are represented by various proxies (Foukal & Lean 1986, 1988; Solanki & Fligge 1998) seeks to avoid this difficulty. Proxies such as the Ca K plage areas (Foukal et al. 2009; Tlatov et al. 2009), the F10.7 microwave index (Tapping 1987), and the Mg II index (Heath & Schlesinger 1986; Fröhlich & Lean 2004) measure emission from the bright chromospheric plages overlying the magnetic features that are visible as WL faculae near the limb. Changes in the areas of these chromospheric plages, or of their disk—integrated emission, were considered to be proportional to changes in the bright component of TSI variation. Some examples of WL faculae and their overlying Ca K plages are shown in Figure 1.

Early photometric studies encouraged this representation of the bright TSI component by chromospheric proxies, since they showed a positive correlation between chromospheric and photospheric brightening in quiet Sun magnetic structures (e.g., Skumanich et al. 1975). More recent photometric imaging supports this correlation for the small magnetic elements of the quiet network, but shows that the contrast of larger plage elements in active network and active region plage is negative near disk center, positive near the limb, and vanishes at intermediate heliocentric angle (e.g., Moran et al. 1992; Zirin & Wang 1992; Lawrence et al. 1993; Topka et al. 1997; Sobotka

et al. 2000; Ortiz et al. 2006). In fact, plage area measurements include even pores and spots that are dark at *all* heliocentric angles (W. Marquette 1992, private communication; Tlatov et al. 2009). So the accuracy of TSI reconstruction based on plage proxies is less clear than has generally been believed.

The sunspot or group number, R , has also been used as a proxy of the bright TSI contribution (Foukal & Lean 1990; Wang et al. 2005; Foukal 2012). Its use has been largely justified by the good correspondence between smoothed values of R and chromospheric proxies like F10.7 (e.g., Foukal & Lean 1990; Foukal 1998a), which can be understood given the loose tendency of plages to accompany spots. But the main reason for its use is the length of the record of R . Spots have been recorded on a regular basis for much longer than have plages or faculae. So whatever its shortcomings, the time series of R provides the only proxy of the bright TSI component prior to 1874.

The most direct measure of the bright TSI component is, in principle, the 102 years record of the WL faculae. Areas of WL faculae measure *only* the bright contribution to TSI without any confusion with photospherically dark structures included in the plage areas or in R . The record of their areas, measured by the Royal Greenwich Observatory (RGO) between 1874 and 1976, has provided new insights into activity prediction (Brown & Evans 1980) and into stellar dynamos (Foukal 1998b). But their limited visibility only near the limb and poorly understood behavior relative to other activity indices have so far prevented much use of the WL facular areas in TSI reconstruction.

In Section 2 we show that a stable relation exists between the time series of Ca K plage and WL facular areas up to moderate activity levels, but it changes during the spot cycles 18 and 19, some of the largest since the 17th century. In Section 3 we propose an explanation of this change. In Section 4 we reconstruct TSI between 1916 and 1976 using the facular areas. In Sections 5 and 6 we describe our results and compare them with previous TSI reconstructions based on plages and on R .

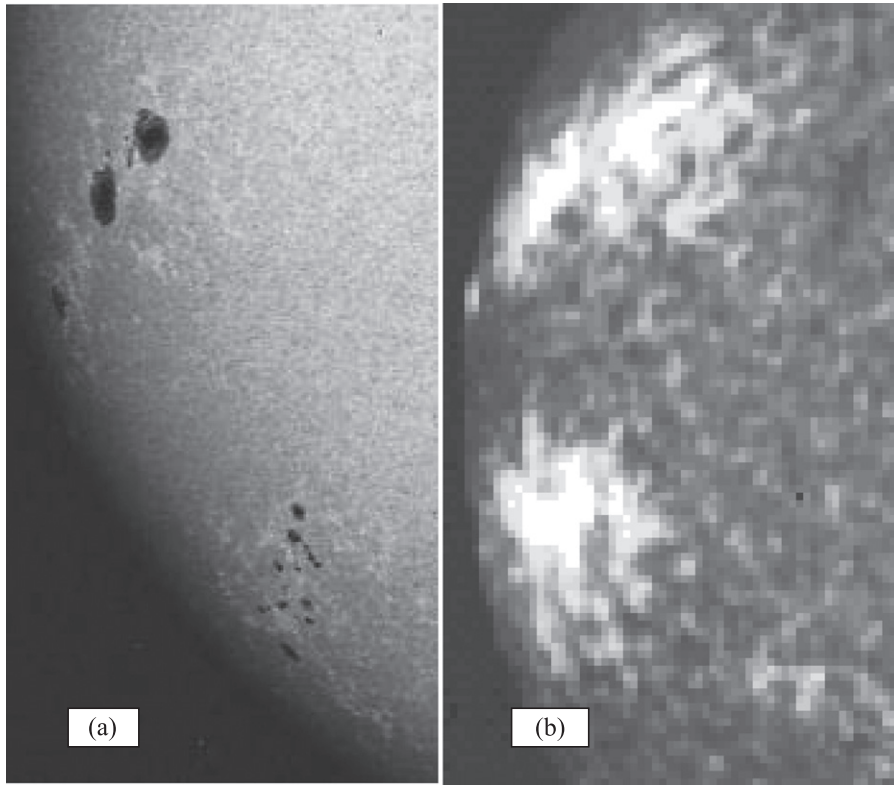


Figure 1. (a) The solar disk imaged in photospheric broadband light and (b) in chromospheric Ca K radiation. WL faculae are seen around the spots in (a); Ca K plages cover them and also most of the sunspots, in (b). Images obtained at Mt. Wilson Observatory on 1957 September 15.

We summarize our results and state our conclusions in Section 7.

2. THE STATISTICAL RELATIONSHIP BETWEEN AREAS OF WL FACULAE AND CA K PLAGES

We use the A_{pn} series of projected plage areas (including surrounding active network) obtained from digitization of the Mt. Wilson Observatory (MWO) and Sacramento Peak Observatory spectroheliograms (Foukal 1998a; Foukal et al. 2009) for the years 1916–1999. The relative variation of annual mean A_{pn} agrees with independent digitization and analysis of the MWO plates by Bertello et al. (2010) and with R .

We use the annual means, A_f , of the projected RGO WL facular areas whose measurement and errors have been discussed elsewhere (Hohenkerk et al. 1967; Brown & Evans 1980; Foukal 1993). The WL faculae are visible only limb-ward of $\theta \sim 35^\circ$, where θ is the heliocentric angle. This presents no disadvantage here since the annual means average over solar rotations.

A plot of the two time series for the overlap period 1916–1976 is shown in Figure 2(a). The relative amplitudes agree for cycles 15, 16, 17, and 20, but the relative amplitudes of the two largest cycles, 18 and 19, in A_{pn} are inverted in A_f .

The relationship between A_f and A_{pn} can be expressed as

$$A_{\text{pn}} = \alpha\beta\gamma(A_f) + \beta(A_s) + \delta, \quad (1)$$

where the projected RGO spot areas, A_s , are introduced because A_{pn} and also the McMath plage index (W. Marquette 1992, private communication) include spot areas.

The geometrical parameter $\alpha \sim 2$ corrects for the limited WL facular zone of visibility ($\theta > 35^\circ$). The parameter $\beta \sim 2.8$,

estimated from measurements on MWO plates, accounts for the larger area of a plage (or spot) in Ca K relative to the corresponding WL structure. The factor $\gamma = \mu d \mu \sim 2.5$ corrects for area projection, where $\mu = \cos \theta$. Finally, δ represents the (small) plage area that may appear at the lowest activity levels when no WL faculae are recorded in the active latitudes (polar facula area is negligible).

Figure 2(b) shows the annual mean A_{pn} compared to its reconstruction from A_f . The reconstructed A_{pn} falls slightly below the observed values of cycles 15–17 and 20 to within the uncertainty in the parameters in relation (1). So a stable and straightforwardly derivable relationship holds up to moderate activity levels. Demonstration of this simple relationship over the 1916–1976 period of overlap between the two time series was not possible before the digitization and reduction of the Ca K spectroheliograms (Foukal 1998a; Tlatov et al. 2009; Bertello et al. 2010). But (1) underestimates the observed A_{pn} in cycles 18 and 19 by about a factor 2.

3. WHY ARE A_{pn} AND A_f INVERSELY RELATED AT HIGH ACTIVITY?

Several factors might, in principle, contribute to this underestimate. For one, A_{pn} includes not only the active region plages but also the surrounding active network (Foukal 1998a). But A_f also includes the active network. This is confirmed by the similarity of A_{pn} and A_f in Figure 2(a) for the four weak to moderate cycles. So neglect of the active network in A_f is not an explanation. A second factor might be the contribution to A_{pn} from the plage area overlying the many small spots that dominate the sunspot number at high activity. But A_s includes

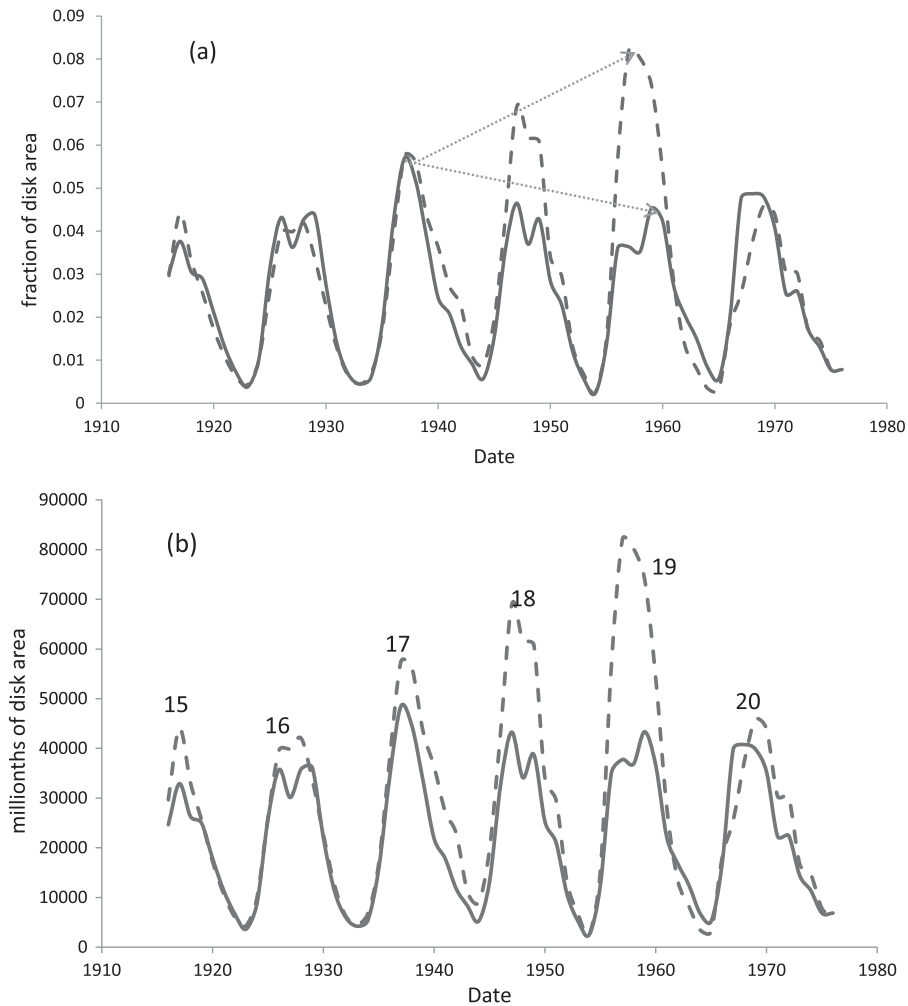


Figure 2. (a) The annual mean A_f (solid) and A_{pn} for sunspot cycles 15–20. A_f has been multiplied by 20. The arrows show the trends of peak A_{pn} and A_f . Panel (b) shows the observed (dashed) and calculated (solid) A_{pn} from relation (1).

group areas down to 2 millionths of the disk (~ 2 arcsec in diameter), so this explanation also cannot be correct.

The most likely explanation is that, at highest activity, a change in the size distribution of flux tubes occurs, decreasing the number of those small enough to appear as WL faculae. Since essentially all solar magnetic structures exhibit bright Ca K (e.g., Skumanich et al. 1975) the greater number of larger flux tubes will increase A_{pn} while A_f decreases.

A transition from bright faculae to dark pores with increasing flux tube cross section is predicted from flux tube dynamics (Spruit 1976). The similarity between the 10%–15% decrease in WL facular area between cycles 17, 18, and 19 seen in Figure 2 and the fractional increase in A_{pn} between those cycles supports this interpretation.

The high resolution measurements of Topka et al. (1997) place this transition between bright and dark magnetic elements near the limb around 1500 G. So a test of this explanation requires the study of the activity dependence of the flux tube size distribution in the range of pores around 0.1–1 arcsec in diameter. Sufficiently stable photometry and spectra polarimetry near the limb over a solar cycle at such resolution remains challenging even for *Hinode* or the Swedish Solar Telescope.

Bogdan et al. (1988) report no change in the flux tube size distribution with activity level. But the sunspot group size measurements they used lack the angular resolution to address

the relevant size range. The data of Ortiz et al. (2006) show no clear decline of bright magnetic elements near the limb, between activity minimum in 1996 and maximum in 2001. But the activity level in 2001 was lower than near the peaks of cycles 18 and 19. Also, the MDI data used in their study again lack the angular resolution to accurately measure micro-pore sized structures near the limb.

Our explanation is supported by the marked increase with activity of the ratio A_s/A_f (Brown & Evans 1980; Foukal 1993). A shift toward lower spatial frequencies in the photospheric field at high activity levels is also consistent with observations of very large spots on younger, more active solar-type stars (e.g., Lockwood et al. 2007) and with recent dynamo calculations (e.g., Tobias et al. 2008).

4. RECONSTRUCTION OF TSI VARIATION USING THE WL FACULAR AREAS

Reconstruction of TSI from A_f proceeds (e.g., Foukal & Lean 1986) by first correcting the radiometrically measured TSI variation, ΔS , for the dimming, P_s , by sunspots. We seek the regression of the corrected values, $\Delta S + P_s$, upon A_f , but the A_f series ended in 1976 and reliable measurements of S became available only in 1980. So we first regress $\Delta S + P_s$ upon A_{pn} . We form annual means of the daily ΔS compiled by Fröhlich

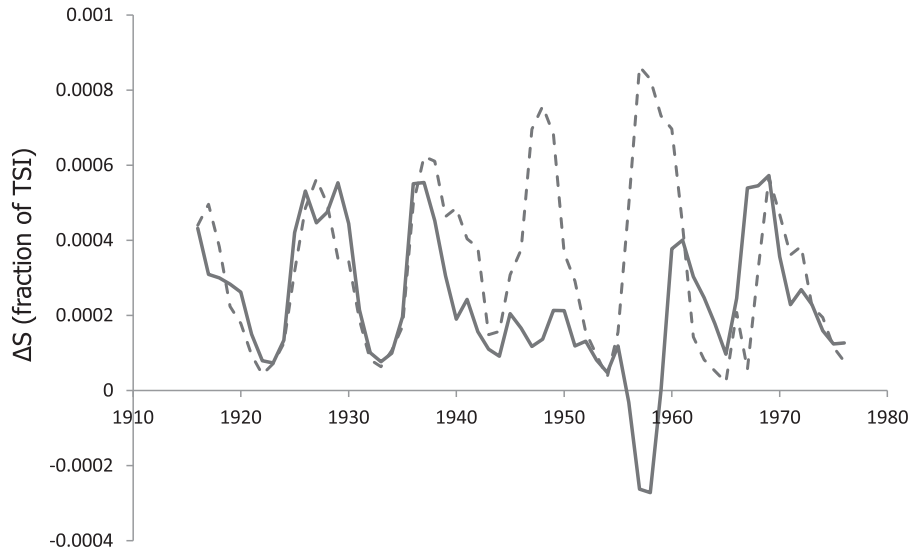


Figure 3. A plot of the annual means of ΔS for 1916–1976 reconstructed from A_f (solid) and from A_{pn} (dashed).

(2012) for the 1980–1999 period when ΔS and A_{pn} are both available.

To correct for spot blocking we add to ΔS the time series of $P_s = 0.33 A_s$ where the factor 0.33 expresses the photometric contrast of a spot. For the period 1980–1999 we use the NOAA/USAF values of A_s multiplied by 1.1 (Foukal 2014). For 1916–1976 we use the RGO values of A_s with the contrast multiplied by 0.8 to correct for the many less-dark small spots included by RGO (Foukal 2014).

Regression of the corrected radiometric time series against A_{pn} yields:

$$\Delta S + P_s = 0.0239A_{pn} - 1 \times 10^{-5} \quad (2)$$

with a correlation coefficient $r = 0.95$.

We then regress A_{pn} upon A_f for the years 1916–1976, when both are available. This yields:

$$A_{pn} = 18.9A_f - 0.0008 \quad (3)$$

with $r = 0.96$.

This linear relation (3) represents the correspondence between photospherically bright structures contributing to A_{pn} and A_f over the period 1916–76. In accordance with the discussion of Section 3 it does not include the change in this relation in cycles 18 and 19. That change is caused by an increase in the relative area of dark photospheric structures that do not contribute to solar brightening, $\Delta S + P_s$. They are observed as plages and contribute to A_{pn} .

Substituting (3) in (2) we obtain:

$$\Delta S + P_s = 0.451A_f + 0.91 \times 10^{-5}. \quad (4)$$

In the substitution of (3) into (2) we assume that the relation between A_f and A_{pn} is stationary between the two periods 1916–1976 and 1980–1999, since they cover a similar range of solar activity. An alternative method for deriving relations (3) and (4) would be to use only years of low to moderate activity in all the cycles. The result is not significantly different.

We now use (4) with A_f to generate the annual means ($\Delta S + P_s$). Finally, we subtract P_s from the time series $\Delta S + P_s$ to form ΔS for 1916–1976.

5. RESULTS

This time series of the TSI variation is shown in Figure 3 together with the TSI reconstructed from A_{pn} . We see that cycles 15, 16, 17, and 20 are in roughly the same proportion reconstructed from A_f and from A_{pn} . But the large maxima of TSI generated in A_{pn} in the late 1940s and 1950s around the peaks of cycles 18 and 19 are absent in the reconstruction from A_f . Instead, TSI begins to dip around 1940 to a minimum in the late 1950s.

If our explanation in Section 3 is correct, the relation (4) between the bright contribution to TSI, $\Delta S + P_s$, and A_f holds at all activity levels. The TSI dip is caused by the increased fraction of the plage elements that are dark in photospheric radiation at the highest activity levels. The decrease with activity level of the ratio A_f/A_s (Brown & Evans 1980; Foukal 1993, 1998b) cannot, on its own, account for the dip since (1) underestimates A_{pn} around the peaks of cycles 18 and 19 even though A_s is included in that reconstruction. So the dip must be caused, as suggested in Section 3, largely by a change in the size distribution of small flux tubes around the transition between bright faculae and dark pores.

Over most of its activity range the Sun falls into the category of stars that brighten at the peak of their spot cycles (e.g., Lockwood et al. 2007). But our findings suggest that, at some of its highest recorded activity levels over the past four centuries the solar dynamo shifted to lower spatial wave numbers so that dimming by spots dominated the brightening by faculae.

6. COMPARISON WITH AN IPCC TSI TIME SERIES AND WITH THE GLOBAL TEMPERATURE RECORD

Figure 4(a) shows a comparison between the TSI reconstructed from A_f and one of the TSI time series used by the Intergovernmental Panel on Climate Change (IPCC). The NRL reconstruction (Wang et al. 2005) uses R to represent the bright contribution. Except for an upward trend caused by a term based on modeling of the turbulent diffusion of photospheric magnetic fields, the NRL series resembles the A_{pn} -based curve in Figure 3; both exhibit peak TSI values around the maxima of

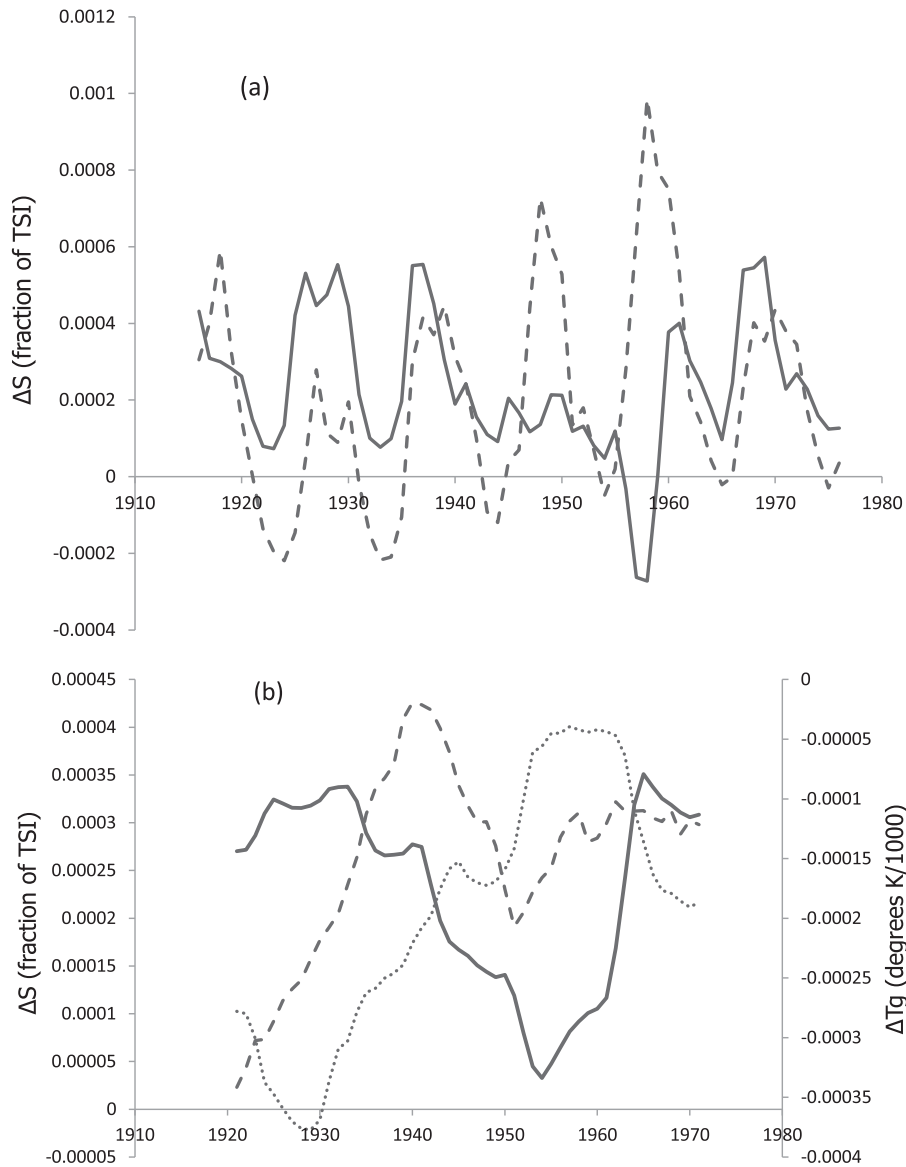


Figure 4. (a) Comparison of ΔS from A_f (solid) and the NRL TSI time series (dashed); (b) 11-year smoothed ΔS from A_f (solid), NRL (dotted) compared to the global temperature variation, T_g (dashed).

cycles 18 and 19 at a time when the A_f -based TSI shows a deep minimum.

Figure 4(b) illustrates the behavior of the 11-year smoothed TSI from A_f and from the NRL model, compared to the HadCRUT global-mean surface air temperature record, T_g (Morice et al. 2012). The onset of the global cooling from the early 1940s through 1960s seen in T_g lags the early 1930s onset of solar dimming derived here by about 10 years. In contrast, the NRL curve exhibits a rise to a TSI maximum in the late 1950s during this global cooling. This suggests that use of the A_f -based curve in climate models may alter the mid-20th century balance between solar, volcanic, aerosol, and greenhouse contributions to global temperature described by the IPCC (e.g., Solomon et al. 2007, p. 190).

7. DISCUSSION AND CONCLUSIONS

The evidence we present here indicates that the Sun *dims* at some of its highest activity levels to TSI values below those of recent solar activity minima. This contradicts the evidence from

past reconstructions, that the Sun *brightened* to some of its highest TSI levels in the past four centuries, around the peaks of cycles 18 and 19. This finding is of particular interest given the recent report (Clette et al. 2014) that high activity comparable to that encountered in cycles 18 and 19 may have occurred also in the mid-18th and 19th centuries. The solar dimming we find in the mid-20th century leads the decrease in global temperatures between the mid-1940s and 1970s by about five years. It will be interesting to investigate possible climate cooling in the mid-18th and 19th century as well.

Our findings do not alter evidence against a dominant solar driving of rapid climate warming since the 1970s (e.g., Solanki & Krivova 2003). They do, however, imply that an increase in future activity beyond cycle 19 levels might dim the Sun by an amount comparable to dimming that may have occurred during the 17th century Maunder Minimum of activity (e.g., Foukal 2012).

Our findings may also help to understand why the Sun is photometrically more quiet than other late-type stars of similar

Ca K variability (Lockwood et al. 2007). We have suggested previously (Foukal 1993, 1994, 1998b) that solar brightening with increased activity is suppressed because a decreasing fraction of the magnetic flux emerges as small, bright flux tubes. This was based on the finding that the ratio, A_s/A_f , of spot (rather than Ca K plage) to WL facular areas increased at high activity levels (Brown & Evans 1980; Foukal 1993). The degree of suppression is likely to vary from star to star because it will depend on the shape of the star's magnetic flux tube size distribution, sensitivity of this shape to activity level, and on the internal structure of its flux tubes. Our finding that the Sun seems to be poised at the transition between stars that brighten with activity and those that darken appears to make it particularly sensitive to such suppression.

This interpretation is supported by the finding that measured daily (but binned) TSI variations increase with R only up to $R \sim 150$ (Solanki & Fligge 1999). Daily values cover a wider range of variation than annual means, so some TSI decrease is revealed in daily data even at the moderate activity levels in cycles 21–24 covered by that study. This suggests that the TSI amplitude of those cycles was suppressed somewhat, but the spot areas in those cycles were too small to cause a dimming as deep and prolonged as during cycles 18 and 19.

Investigation using monthly data may provide further tests of the mechanism proposed here to limit A_f , and so cause solar dimming. But such investigation must take into account that the ratio A_f/A_s is not uniquely determined by the activity level on any day within a given cycle. Remarkably, it depends also on the amplitude of that cycle (Brown & Evans 1980; Foukal 1993). Unfortunately, the record of A_f was discontinued in 1976. Given the importance of WL faculae, it would be desirable to renew this record using observations from, e.g., the Precision Solar Photometric Telescopes (PSPT's).

This study relied on the compilations of sunspot statistics maintained by D. Hathaway at the NASA Marshall Space Flight Center, on the RGO spot and facular data archived by the UK Solar System Data Center, and on the MWO/CRI Ca K images available from the NOAA/SEL World Data Center.

I thank C. Fröhlich for comments on the paper and R. Ulrich for providing Figure 1(b). I am so grateful to the referee for several useful suggestions.

REFERENCES

- Bertello, L., Ulrich, R., & Boyden, J. 2010, *SoPh*, 264, 31
 Bogdan, T., Gilman, P., Lerche, I., & Howard, R. 1988, *ApJ*, 327, 451
 Brown, G., & Evans, D. 1980, *SoPh*, 66, 233
 Clette, F., Svalgaard, L., Vacquero, J., & Cliver, E. 2014, *SSRv*, 186, 35
 Foukal, P. 1993, *SoPh*, 148, 219
 Foukal, P. 1994, *Sci*, 264, 238
 Foukal, P. 1998a, *GeoRL*, 25, 2909
 Foukal, P. 1998b, *ApJ*, 500, 958
 Foukal, P. 2012, *SoPh*, 279, 365
 Foukal, P. 2014, *SoPh*, 289, 1517
 Foukal, P., Bertello, L., Livingston, W., et al. 2009, *SoPh*, 255, 229
 Foukal, P., & Lean, J. 1986, *ApJ*, 302, 836
 Foukal, P., & Lean, J. 1988, *ApJ*, 328, 347
 Foukal, P., Little, R., Graves, J., Rabin, D., & Lynch, D. 1990, *ApJ*, 353, 712
 Fröhlich, C. 2012, *SGeo*, 33, 453
 Fröhlich, C., & Lean, J. 2004, *ARA&A*, 12, 273
 Heath, D., & Schlesinger, B. 1986, *JGR*, 91, 8672
 Hohenkerk, C., Ladley, C., & Rudd, P. 1967, *ROAn*, 11, 5
 Lawrence, J., Topka, K., & Jones, H. 1993, *JGR*, 98, 18911
 Lockwood, W., Skiff, B., Henry, G., et al. 2007, *ApJS*, 171, 260
 Moran, T., Foukal, P., & Rabin, D. 1992, *SoPh*, 142, 35
 Morice, C., Kennedy, J., Rayner, N., Jones, P. & HadCRUT 2012, *JGR*, 117, 2012
 Ortiz, A., Domingo, V., & Sanahuja, B. 2006, *A&A*, 452, 311
 Skumanich, A., Smythe, C., & Frazier, E. 1975, *ApJ*, 200, 747
 Sobotka, M., Vazquez, M., Sanchez Cuberes, M., Bonet, J., & Hanslmeier, A. 2000, *ApJ*, 544, 1155
 Solanki, S., & Fligge, M. 1998, *GeoRL*, 25, 341
 Solanki, S., & Fligge, M. 1999, *GeoRL*, 26, 2465
 Solanki, S., & Krivova, N. 2003, *JGR*, 108, 1200
 Solomon, S., et al. IPCC 2007, *The Physical Science Basis* (Cambridge: Cambridge Univ. Press)
 Spruit, H. 1976, *SoPh*, 50, 269
 Tapping, K. 1987, *JGR*, 92, 829
 Tlatov, A., Pevtsov, A., & Singh, J. 2009, *SoPh*, 255, 239
 Tobias, S., Cattaneo, F., & Brummel, N. 2008, *ApJ*, 685, 596
 Topka, K., Tarbell, E., & Title, A. 1997, *ApJ*, 484, 479
 Wang, Y.-M., Lean, J., & Sheeley, N. 2005, *ApJ*, 625, 522
 Zirin, H., & Wang, M. 1992, *ApJL*, 385, L27